THE ASTROPHYSICAL JOURNAL, 450:289–301, 1995 September 1

RADIO CONTINUUM MEASUREMENTS OF SOUTHERN EARLY-TYPE STARS

CLAUS LEITHERER,[1] JESSICA M. CHAPMAN,[2] AND BÄRBEL KORIBALSKI[3]
Received 1995 February 10; accepted 1995 March 16

ABSTRACT

We report the results of a pilot project to measure radio continuum flux densities of early-type stars with the Australia Telescope Compact Array. A sample of 12 stars comprising six Wolf-Rayet stars, three B hypergiants, two Of stars, and one luminous blue variable has been observed at 8.64 GHz and 4.80 GHz. Eleven objects have been detected at 8.64 GHz and seven at 4.80 GHz, respectively. All objects except the luminous blue variable HD 168625 were unresolved at an angular resolution of 1″, as expected if the radio flux originates in dense, ionized stellar winds. HD 168625 is clearly resolved; we detect an incomplete circumstellar ring whose morphology is rather similar to the Hα morphology of the nebula discovered by Hutsmékers et al.

The radio spectrum between 8.64 GHz and 4.80 GHz of all sources detected at both frequencies is consistent with thermal emission from an optically thick wind expanding at constant velocity. The radio fluxes are used to derive accurate mass-loss rates. We find very similar mass-loss rates for the six Wolf-Rayet stars of type WNL in our sample: $\dot{M} \approx 10^{-4.3\pm0.15}\ M_\odot\ \mathrm{yr}^{-1}$, supporting previous results of a very small dispersion among the mass-loss rates of WNL stars. Comparison with rates determined from optical recombination lines suggests excellent agreement. This result makes it unlikely that *distance-dependent* density inhomogeneities are present in the winds.

Our data essentially double the number of luminous B stars detected in the radio. The mass-loss rates of the three B hypergiants are among the most accurate ever derived for B stars. Their rates are not correlated with luminosity. The massive O3 V((f)) star HD 93250 has only been detected at 8.64 GHz. The mass-loss rate required to account for the measured radio flux is $\dot{M} \approx 10^{-4.39\pm0.15}\ M_\odot\ \mathrm{yr}^{-1}$. This rate is several times higher than expected on the basis of its Hα luminosity. We speculate that most of the 8.64 GHz flux is nonthermal and that the true mass-loss rate, for this source, is lower than implied by thermal emission alone.

Subject headings: radio continuum: stars — stars: early-type — stars: mass loss — stars: Wolf-Rayet

1. INTRODUCTION

Hot luminous stars develop strong stellar winds with terminal velocities in excess of the photospheric surface escape velocity (Cassinelli & Lamers 1987; Willis & Garmany 1987). The resulting mass-loss rates $\dot{M}$ are high enough to decrease the stellar mass significantly on an evolutionary timescale. Together with the mass and the chemical composition, $\dot{M}$ is the single most important parameter governing the evolution of massive, early-type stars (Maeder 1994). For the purpose of this paper we will include O stars, luminous blue variables (LBVs), and Wolf-Rayet (W-R) stars in this stellar class. General properties of O stars are discussed by Conti & Underhill (1988). W-R stars are the evolved, chemically enriched descendants of O stars. A comprehensive review of this stellar category has been given by Abbott & Conti (1987). LBVs are believed to be a short evolutionary episode of stars intermediate between types O and W-R. Their properties have been summarized by Davidson, Moffat, & Lamers (1989).

Determination of accurate mass-loss rates is far from trivial, and even the best mass-loss rates available have uncertainties of about 0.2 dex (Lamers & Leitherer 1993). Mass-loss rates of hot, massive stars have traditionally been derived in three fundamental ways: (i) from optical recombination line radiation; (ii) from P Cygni profiles of highly ionized metal lines in the space ultraviolet; and (iii) from thermal bremsstrahlung at infrared and radio wavelengths.

From an observational point of view, deriving $\dot{M}$ from recombination lines is the most straightforward method. Unfortunately, even the strongest lines, such as Hα, originate relatively deep at the base of the wind where the material is undergoing a rapid acceleration. Interpretation of the observed line profiles requires knowledge of the velocity field $v(r)$ of the outflow. One can determine $v(r)$ from a comparison of the observed line profiles and detailed non-LTE line modeling. This approach has been successfully used for W-R stars (e.g., Hamann 1994) and LBVs (Scuderi et al. 1994), which have very strong winds. In contrast, wind densities in O stars are often too small, and their Hα opacities are too low to permit line profile fits. In this case, an assumption for the shape of $v(r)$ must be made to derive $\dot{M}$ (Lamers & Leitherer 1993). For all categories of stars discussed here, some theoretical modeling is required to extract mass-loss rates from measurements of Hα, either by computing theoretical profiles with model atmospheres (Sellmaier et al. 1993) or by solving the radiation-hydrodynamics of the outflow and predicting the appropriate velocity field (Pauldrach 1987; Schaerer & Schmutz 1994).

Observations of ultraviolet resonance lines of, e.g., C IV λ1550 or Si IV λ1400 provide the means to circumvent the uncertainty of the velocity field. These lines originate far from the base of the wind, where radiative and gravitational forces are negligible. As a result, the wind velocity has reached its asymptotic, constant value v_∞, which can easily be determined from the blueshift of the line (Prinja, Barlow, & Howarth 1990). The number of mass-loss determinations from ultraviolet lines peaked in the early years after the launch of the *IUE*

[1] Space Telescope Science Institute, 3700 San Martin Drive, Baltimore, MD 21218; leitherer@stsci.edu.
[2] Anglo-Australian Observatory, P.O. Box 296, Epping, NSW 2121, Australia; jmc@aaoepp.aao.gov.au.
[3] Australia Telescope National Facility, CSIRO, P.O. Box 76, Epping, NSW 2121, Australia; bkoribal@atnf.csiro.au.

satellite (e.g., Garmany et al. 1981). Unfortunately, this method is inherently uncertain due to the required knowledge of the chemistry and ionization state of the wind, which must be both determined in order to derive $\dot{M}$. Lamers & Groenewegen (1990) demonstrated that theoretical models cannot account for the observed ionization of these elements. Since observations of ultraviolet lines always give the product of mass-loss rate and ionization fraction, $\dot{M}$ cannot be obtained without utilizing another, independent method. As a result, ultraviolet resonance lines are hardly used any longer to determine $\dot{M}$. They are, however, crucial for obtaining v_∞.

Hydrogen in winds from hot stars is fully ionized. The plasma emits a characteristic spectrum due to thermal bremsstrahlung (Wright & Barlow 1975; Panagia & Felli 1975; Olnon 1975). The spectrum can be observed in the radio region, where the radiation is optically thick, and in the infrared, where the radiation approaches optical depth zero and becomes indistinguishable from photospheric emission. For the latter reason [and due to the added difficulty of the $v(r)$ dependence], infrared observations are rarely used to determine $\dot{M}$, except for objects with extremely dense winds (e.g., Barlow, Smith, & Willis 1981). On the other hand, radio measurements at centimeter wavelengths provide the most reliable mass-loss rates (Abbott et al. 1980, 1986; Abbott, Bieging, & Churchwell 1981; Bieging, Abbott, & Churchwell 1989). The simplicity of the radiative transfer of the free-free emission process introduces few model assumptions for the determination of $\dot{M}$. If the outflow is stationary, homogeneous, and spherically symmetric—conditions which are usually assumed, regardless of the mass-loss method, then $\dot{M}$ and the radio flux are related by a simple *analytical* formula. Radio measurements of $\dot{M}$ are sometimes even taken to calibrate other techniques, such as measurements of Hα fluxes in order to constrain the unknown velocity law (Leitherer 1988), or observations of ultraviolet resonance lines in order to calibrate the ionization state (Lamers 1981). In fact, most of our knowledge of mass-loss rates from hot stars ultimately relies on radio data. Unfortunately, typical flux densities limit the number of possible detections. Bieging et al. (1989) published a complete survey of all OB stars accessible from the north with the Very Large Array (VLA).[4] The total number of detections is only about 15, and it is not expected that this number will increase dramatically in the near future.

A very small number of hot stars in the southern sky have been observed at radio wavelengths. Leitherer & Robert (1991) obtained 1.3 mm measurements of a sample of O and W-R stars with the Swedish ESO Submillimeter Telescope (SEST). Few additional stars are within the present flux limits of this telescope. Hardly any centimeter data of southern stars which could be used to study their stellar winds are available. Hot stars are embedded in H II regions which confuse the stellar signal at centimeter wavelengths when observed with single-dish instruments. With the availability of the Australia Telescope Compact Array (ATCA), it has become feasible to extend the survey of northern hot stars by the VLA to the south. The southern hemisphere is particularly attractive for such observations, since some of the most massive stars with the highest mass-loss rates are in the Carina region.

In this paper we report the results of a pilot project to observe hot stars with the ATCA at 8.64 GHz and 4.80 GHz. Our goal is to establish the feasibility of such a project and to determine accurate mass-loss rates utilizing the measured radio fluxes.

[4] The VLA of the National Radio Astronomy Observatory is operated by the Association of Universities for Research in Astronomy Inc., under contract with the NSF.

2. OBSERVATIONS AND DATA ANALYSIS

We selected a sample of 12 southern early-type stars with declinations below $-15°$. To maximize the chances of detecting radio continuum emission, we selected sources for which we predicted that the 6 and 3 cm radio flux densities would be above 0.5 mJy at 3 cm. The expected radio flux densities were estimated using values of the stellar distances, mass-loss rates, wind velocities, and chemical compositions given in the literature.

The observations were taken on 1994 September 7–9 using the Australia Telescope Compact Array (ATCA) with a maximum baseline of 6 km. The ATCA is a synthesis instrument consisting of six 22 m antennas on an east-west track, located near Narrabri in New South Wales. The selected source were simultaneously observed in two frequency bands centered at 8.64 GHz (3 cm) and 4.80 GHz (6 cm) with a bandwidth in each case of 128 MHz. To obtain reasonable u-v coverages, each source was observed for a total time of 2 hr, split into six slots of 20 minutes, distributed over the LST range of the source. The sources were corrected for atmospheric amplitude and phase variations using observations of nearby strong continuum sources, and the flux density scale was calibrated using the source 1934−638 as a primary calibrator which was taken to have 6 and 3 cm flux densities of 5.83 and 2.84 Jy, respectively.

The data reduction was carried out in a standard way using the AIPS software package at the Australia Telescope National Facility (ATNF). After editing and calibrating the data, the source visibilities were Fourier transformed using "natural weighting." The images were CLEANed (Högbom 1974; Clark 1980) and restored with a synthesized beam of approximately 1″ and 2″ at 8.64 and 4.80 GHz, respectively. The restoring beam used for each source is displayed in the bottom left hand corner of each contour plot (Figs. 1–18). We show only those maps with detections at either frequency.

We detected radio continuum emission at 3 cm (8.64 GHz) from 11 of the 12 stars in our sample. Seven of these sources were also detected at 6 cm. Only one source, HD 152836, was undetected at either frequency. With the exception of the luminous blue variable HD 168625, the radio emission was unresolved at both frequencies. For the unresolved sources, we have obtained radio positions and flux densities by fitting two-dimensional Gaussian components to the radio images. The noise levels in the images were estimated by measuring the rms levels in a region near the source. At 3 cm the 1 σ level was typically 0.1 mJy. At 6 cm the 1 σ levels were higher, between 0.1 and 1.3 mJy. The poorer sensitivity of the 6 cm images arises from the background confusion of distant sources.

The results are given in Table 1, which lists the radio (8.64 GHz) and optical positions and the measured flux densities at 8.64 and 4.80 GHz. The flux density errors quoted are 1 σ for detections and 3 σ for upper limits. HD 152836 was not detected at either frequency, and only the optical position is given. HD 168625 was not detected at 4.80 GHz, and we list its 3 σ upper limit in Table 1. HD 168625 was clearly resolved at 8.64 GHz (Fig. 18). A discussion of the radio properties is given in § 3. The 4.8 GHz image of this source showed strong confusion. With the limited u-v coverage of our observations, we were unable to distinguish possible extended source structure

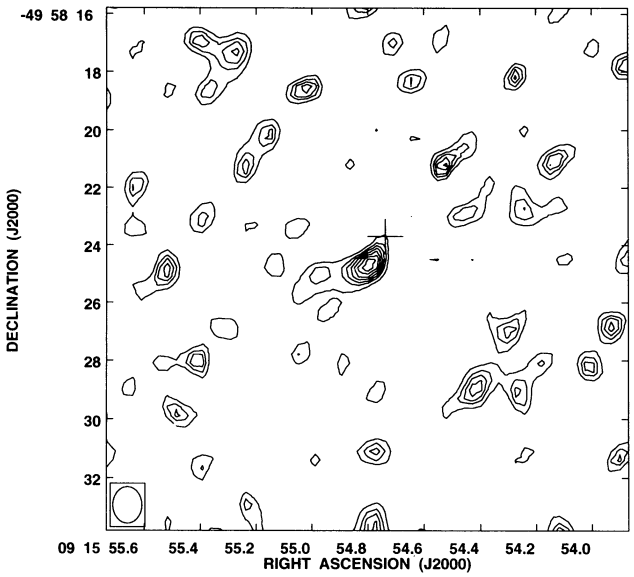

FIG. 1.—Contour map of 8.64 GHz emission of HD 80077. Contour intervals are 0.128, 0.205, 0.256, 0.307, 0.356, 0.410, and 0.461 mJy per beam area. Beam size is indicated in the lower left corner. The map is centered on the observed 8.64 GHz position. The cross marks the optical position.

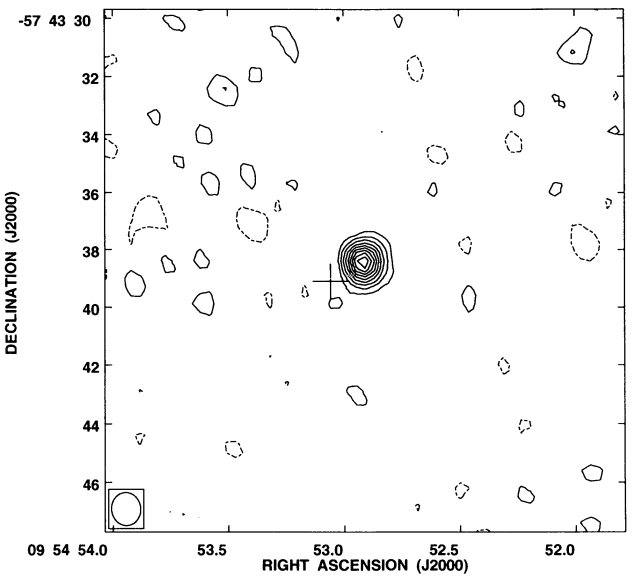

FIG. 3.—Contour map of 8.64 GHz emission of HD 86161. Negative contours are dashed. Contour intervals are −0.166, 0.166, 0.333, 0.499, 0.666, 0.832, 0.998, 1.16, 1.33, and 1.50 mJy per beam area. Beam size is indicated in the lower left corner. The map is centered on the observed 8.64 GHz position. The cross marks the optical position.

from background confusion. A longer observation with improved *u-v* coverage is needed at this frequency. We therefore do not discuss the 4.8 GHz image further in this paper.

The radio positions in Table 1 have precisions of ±0″.15 in each coordinate. The optical positions are less accurate and were taken from the SAO catalog, apart from LSS 4065, which is not an SAO star. Its position was measured on a *Hubble Space Telescope* (*HST*) Guide Star Catalog plate. The SAO positions have declination dependent precisions, with a mean value for declinations between 0 and −60° of 0″.8 (Russell et al. 1990). For all sources, apart from HD 168625, the radio and optical positions are in agreement within the expected errors.

3. THE CIRCUMSTELLAR NEBULA AROUND HD 168625

We begin our discussion with HD 168625, the only resolved source in our sample. HD 168625 is a bona fide member of the LBV class. LBVs experience sudden outbursts sometimes leading to the ejection of massive *spatially resolved* circumstellar shells (Davidson 1989). Such shells have been found among several LBVs. Hutsemékers et al. (1994) detected a ringlike

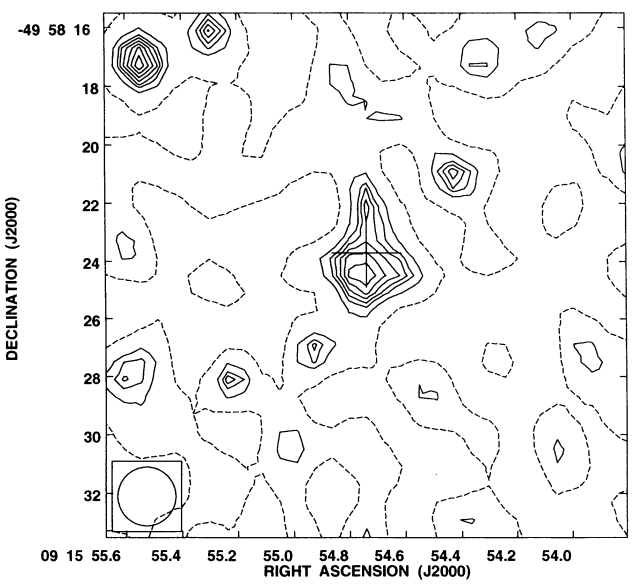

FIG. 2.—Contour map of 4.80 GHz emission of HD 80077. Zero contours are dashed. Contour intervals are 0.0000, 0.127, 0.170, 0.191, 0.212, 0.233, 0.255, and 0.276 mJy per beam area. Beam size is indicated in the lower left corner. The map is centered on the observed 4.80 GHz position. The cross marks the optical position.

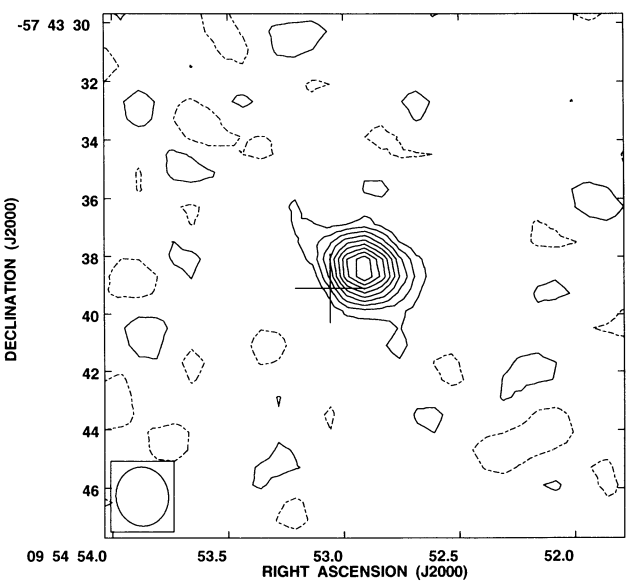

FIG. 4.—Contour map of 4.80 GHz emission of HD 86161. Negative contours are dashed. Contour intervals are −0.117, 0.117, 0.233, 0.350, 0.466, 0.583, 0.699, 0.816, 0.933, and 1.05 mJy per beam area. Beam size is indicated in the lower left corner. The map is centered on the observed 4.80 GHz position. The cross marks the optical position.

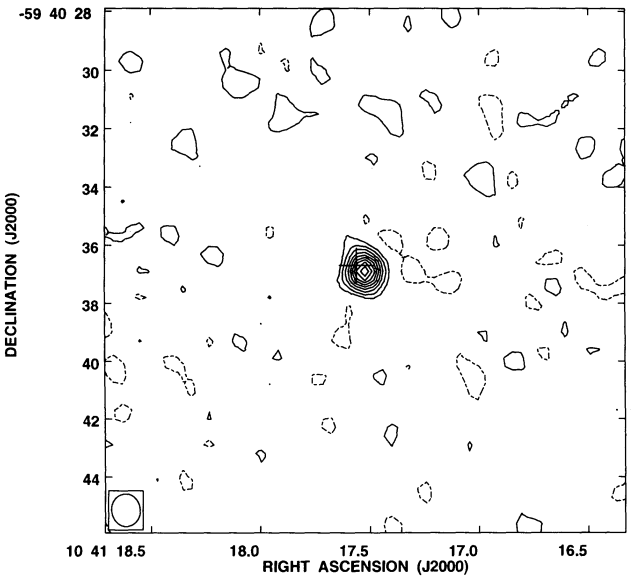

FIG. 5.—Contour map of 8.64 GHz emission of HD 92740. Negative contours are dashed. Contour intervals are −0.153, 0.153, 0.305, 0.458, 0.611, 0.764, 0.916, 1.07, 1.22, and 1.37 mJy per beam area. Beam size is indicated in the lower left corner. The map is centered on the observed 8.64 GHz position. The cross marks the optical position.

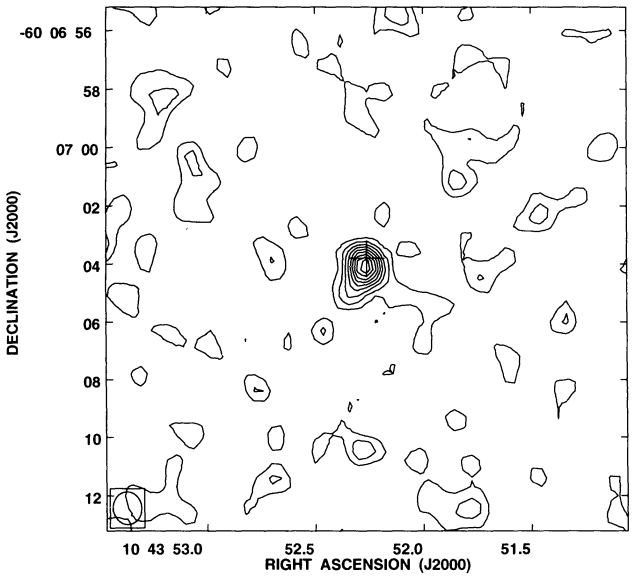

FIG. 7.—Contour map of 8.64 GHz emission of HD 93131. Contour intervals are 0.0945, 0.189, 0.284, 0.378, 0.473, 0.567, 0.662, 0.756, and 0.851 mJy per beam area. Beam size is indicated in the lower left corner. The map is centered on the observed 8.64 GHz position. The cross marks the optical position.

nebula around HD 168625. The nebular mass amounts to a few percent of a solar mass. No such nebula was detected by these authors around HD 168607, another LBV, in a search using the same technique as for HD 168625.

The 3 cm image of HD 168625, reproduced in Figure 18, shows an incomplete shell-like structure, with extended emission over a region of 20″ × 18″, measured north-south, by east-west. The total emission detected within this region was 14 ± 2 mJy. The strongest emission was detected from two components, located 4″.5 to the west and south of the stellar positions. Table 2 gives the positions and peak fluxes for these components.

The morphology and size of the nebula in the radio and in Hα (Hutsemékers et al. 1994) are remarkably similar. Both the radio and optical images show stronger emission to the south and west of the optical position, with weaker emission extending to the northeast. Our 3 cm image overlays with the inner elliptical ring described by Hutsemékers et al. (1994). The

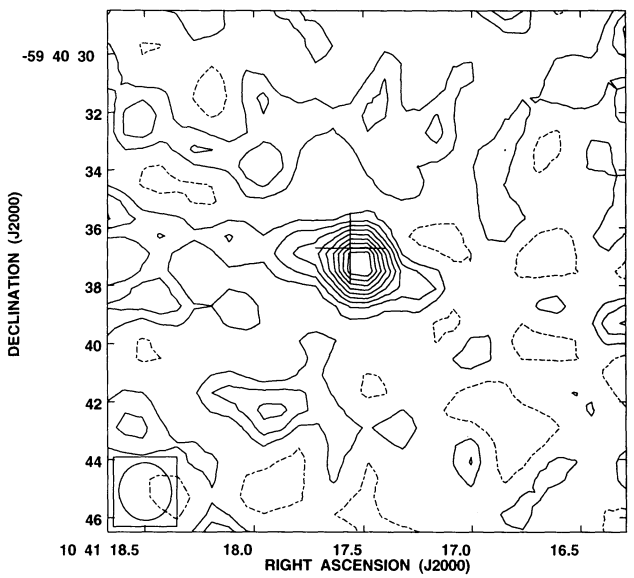

FIG. 6.—Contour map of 4.80 GHz emission of HD 92740. Negative contours are dashed. Contour intervals are −0.130, 0.130, 0.260, 0.390, 0.521, 0.651, 0.781, 0.911, 1.04, and 1.17 mJy per beam area. Beam size is indicated in the lower left corner. The map is centered on the observed 4.80 GHz position. The cross marks the optical position.

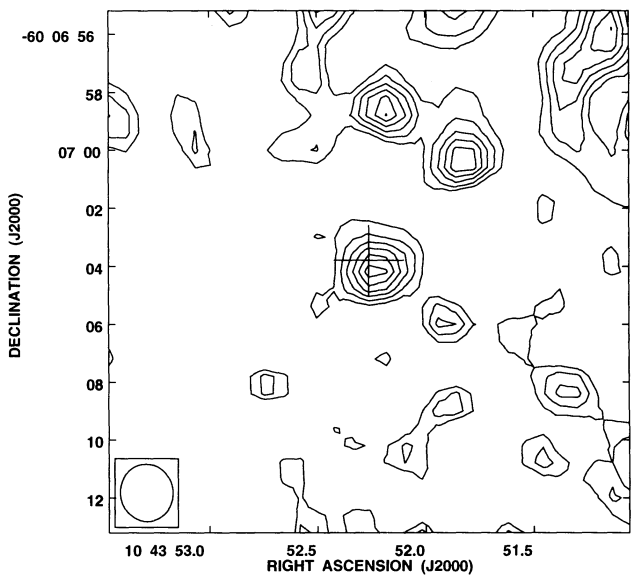

FIG. 8.—Contour map of 4.80 GHz emission of HD 93131. Contour intervals are 0.0578, 0.116, 0.173, 0.231, 0.289, and 0.347 mJy per beam area. Beam size is indicated in the lower left corner. The map is centered on the observed 4.80 GHz position. The cross marks the optical position.

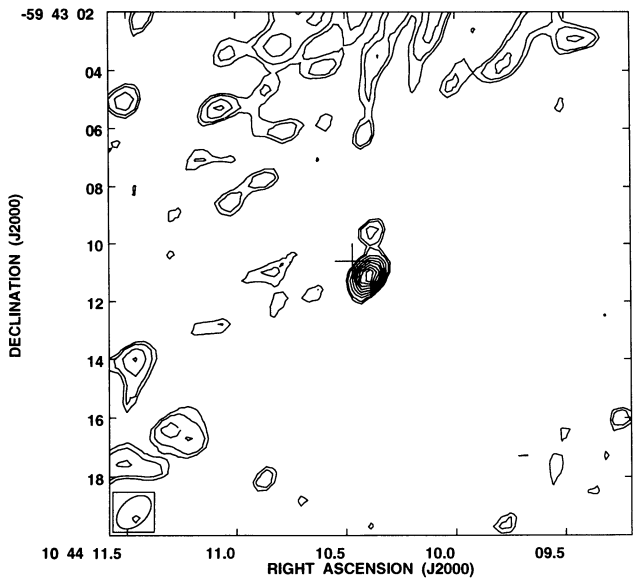

FIG. 9.—Contour map of 8.64 GHz emission of HD 93162. Contour intervals are 0.157, 0.210, 0.315, 0.419, 0.524, 0.629, 0.734, 0.839, and 0.944 mJy per beam area. Beam size is indicated in the lower left corner. The map is centered on the observed 8.64 GHz position. The cross marks the optical position.

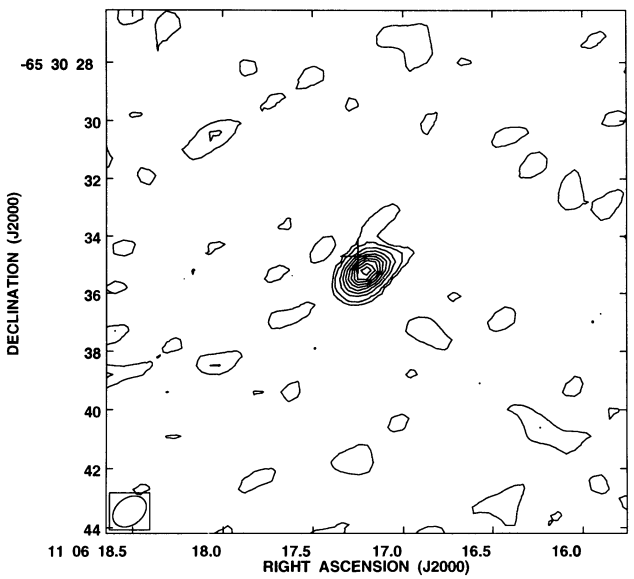

FIG. 11.—Contour map of 8.64 GHz emission of HD 96548. Contour intervals are 0.123, 0.247, 0.494, 0.740, 0.987, 1.23, 1.48, 1.73, 1.97, and 2.22 mJy per beam area. Beam size is indicated in the lower left corner. The map is centered on the observed 8.64 GHz position. The cross marks the optical position.

similar morphologies suggest that interstellar extinction is not significantly variable across the area of the nebula.

The dereddened Hα flux of the nebula measured by Hutsemékers et al. (1994) is between 2.5×10^{-12} ergs s^{-1} cm^{-2} and 1.2×10^{-11} ergs s^{-1} cm^{-2}, depending on $E(B-V)$, which is quite uncertain. Israel & Kennicutt (1980) calculated the ratio of the thermal flux at 8.64 GHz over the flux in Hα for standard case B recombination. Using their relation we predict a thermal flux of $S_\nu^{8.64} \approx 1.5$–7 mJy from the Hα flux observed by Hutsemékers et al. (1994). The total flux of the two main sources in Table 2 agrees reasonably well with the prediction. This suggests that the observed 8.64 GHz flux corresponds entirely to thermal, optically thin emission from the circumstellar nebula.

4. THERMAL EMISSION FROM STELLAR WINDS

The theoretical radio spectrum of an expanding stellar wind has been derived by Panagia & Felli (1975) and Wright & Barlow (1975). They showed that the measured radio flux can

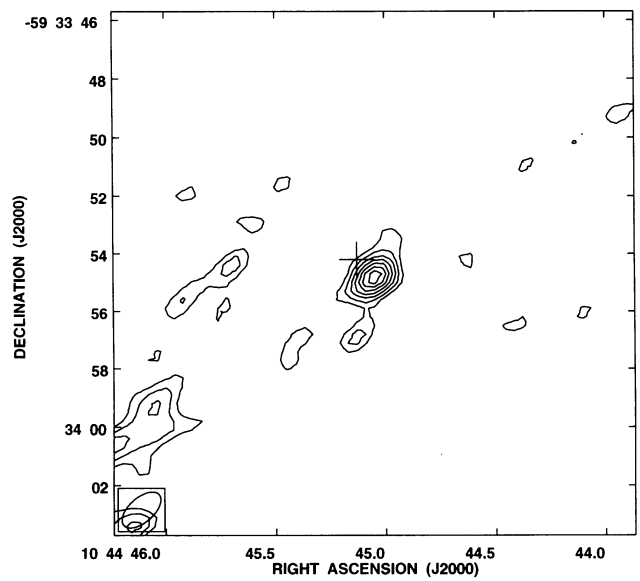

FIG. 10.—Contour map of 8.64 GHz emission of HD 93250. Contour intervals are 0.338, 0.451, 0.563, 0.676, 0.789, 0.901, and 1.01 mJy per beam area. Beam size is indicated in the lower left corner. The map is centered on the observed 8.64 GHz position. The cross marks the optical position.

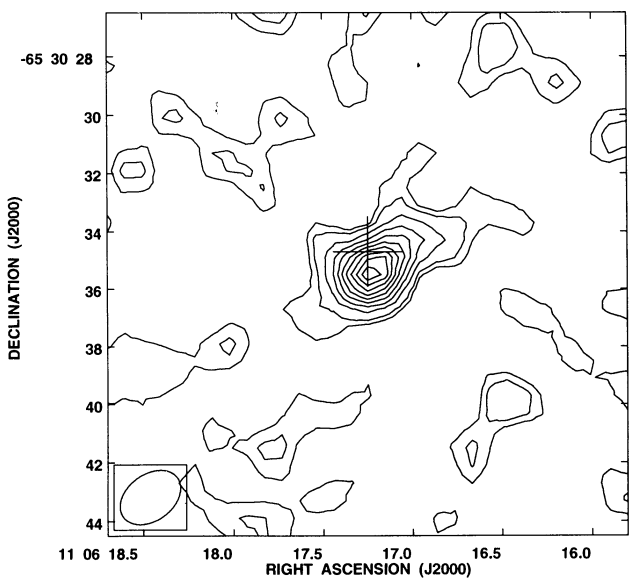

FIG. 12.—Contour map of 4.80 GHz emission of HD 96548. Contour intervals are 0.0814, 0.163, 0.326, 0.488, 0.651, 0.814, 0.977, 1.14, 1.30, and 1.47 mJy per beam area. Beam size is indicated in the lower left corner. The map is centered on the observed 4.80 GHz position. The cross marks the optical position.

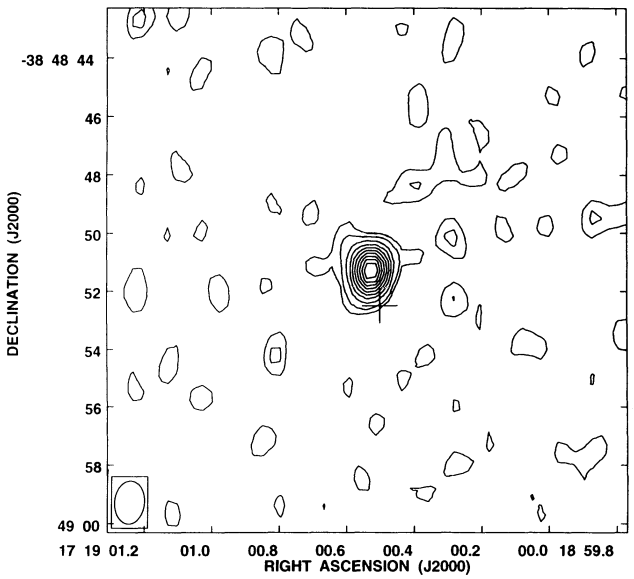

FIG. 13.—Contour map of 8.64 GHz emission of LSS 4065. Contour intervals are 0.143, 0.285, 0.570, 0.855, 1.14, 1.43, 1.71, 2.00, 2.28, and 2.57 mJy per beam area. Beam size is indicated in the lower left corner. The map is centered on the observed 8.64 GHz position. The cross marks the optical position.

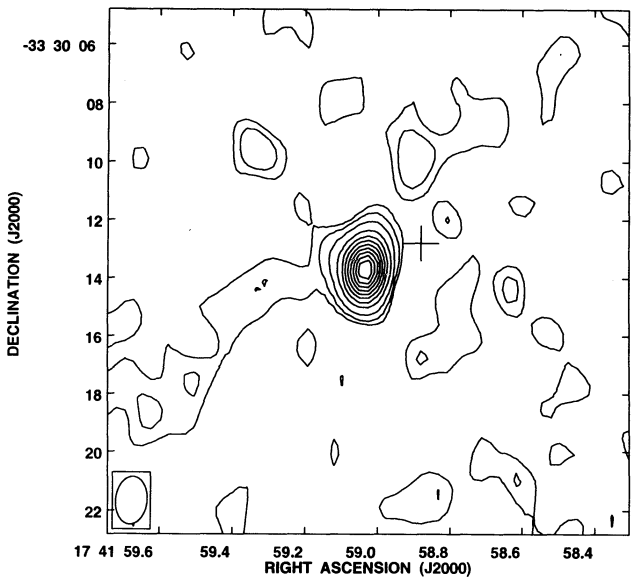

FIG. 15.—Contour map of 8.64 GHz emission of HD 160529. Contour intervals are 0.117, 0.234, 0.468, 0.936, 1.40, 1.87, 2.34, 2.81, 3.28, 3.74, and 4.21 mJy per beam area. Beam size is indicated in the lower left corner. The map is centered on the observed 8.64 GHz position. The cross marks the optical position.

be related to the stellar-wind density by

$$S_\nu = 2.32 \times 10^4 \left(\frac{\dot{M} Z}{v_\infty \mu}\right)^{4/3} \left(\frac{\gamma g_\nu \nu}{d^3}\right)^{2/3} . \quad (1)$$

S_ν is the flux density in mJy, ν is the frequency in Hz, d is the distance in kpc, $\dot{M}$ is in $M_\odot$ yr^{-1}, and v_∞ is in km s^{-1}; μ, Z, and γ are the mean molecular weight, the rms ionic charge, and the mean number of electrons per ion, respectively. If A_i, M_i, and Z_i are the fractional abundance, molecular weight, and ionic charge of the ith atomic/ionic species, μ, Z, and γ are defined as:

$$\mu = \frac{\sum A_i M_i}{\sum A_i}, \quad Z = \frac{(\sum A_i Z_i^2)^{1/2}}{\sum A_i}, \quad \gamma = \frac{\sum A_i Z_i}{\sum A_i} . \quad (2)$$

g_ν is the free-free Gaunt factor. We approximate g_ν with

$$g_\nu = 9.77\left(1 + 0.13 \log \frac{T_e^{3/2}}{Z\nu}\right), \quad (3)$$

where T_e[K] is the electron temperature of the wind, and ν is in

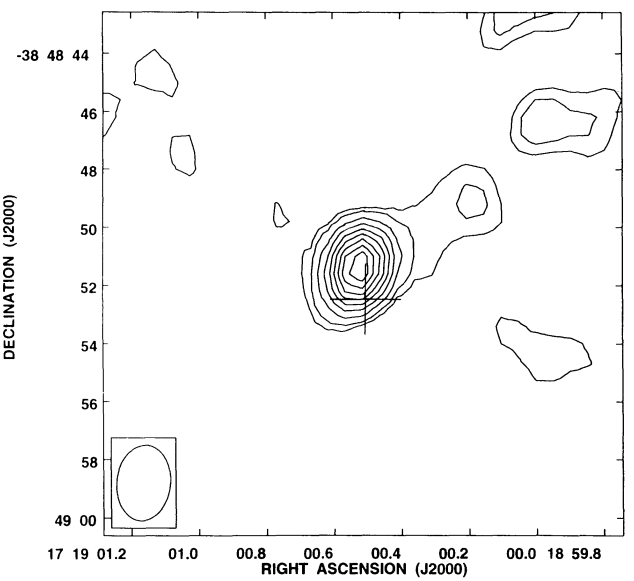

FIG. 14.—Contour map of 4.80 GHz emission of LSS 4065. Contour intervals are 0.276, 0.368, 0.552, 0.736, 0.920, 1.10, 1.29, 1.47, and 1.66 mJy per beam area. Beam size is indicated in the lower left corner. The map is centered on the observed 4.80 GHz position. The cross marks the optical position.

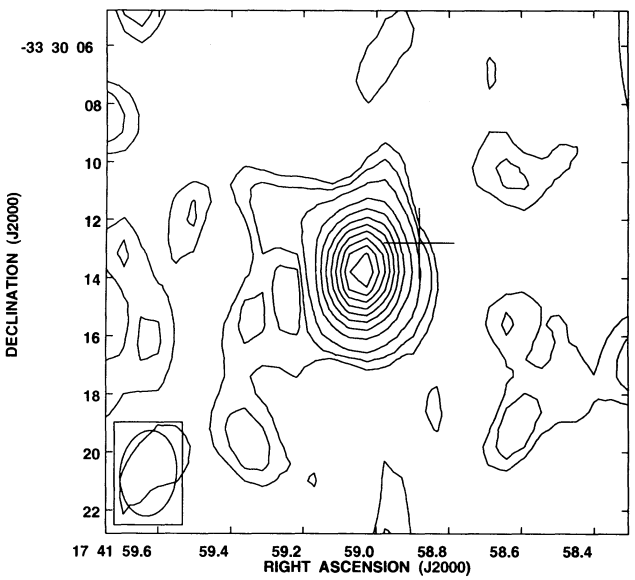

FIG. 16.—Contour map of 4.80 GHz emission of HD 160529. Contour intervals are 0.0869, 0.174, 0.347, 0.695, 1.04, 1.39, 1.74, 2.08, 2.43, 2.78, and 3.13 mJy per beam area. Beam size is indicated in the lower left corner. The map is centered on the observed 4.80 GHz position. The cross marks the optical position.

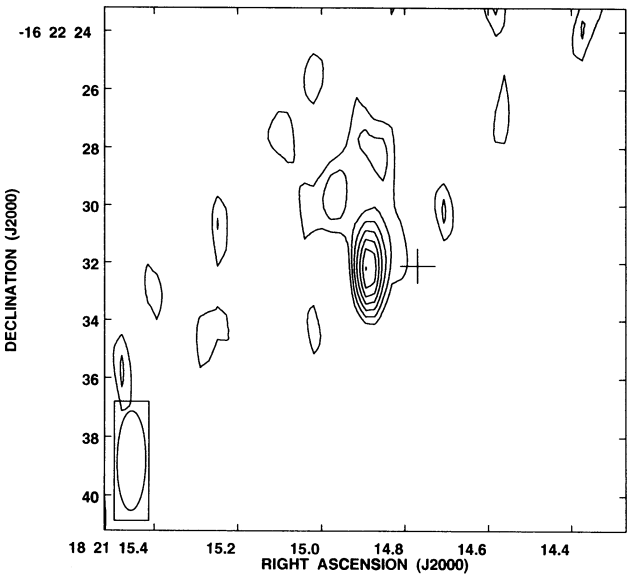

FIG. 17.—Contour map of 8.64 GHz emission of HD 168607. Contour intervals are 0.262, 0.349, 0.437, 0.524, 0.611, 0.699, and 0.786 mJy per beam area. Beam size is indicated in the lower left corner. The map is centered on the observed 8.64 GHz position. The cross marks the optical position.

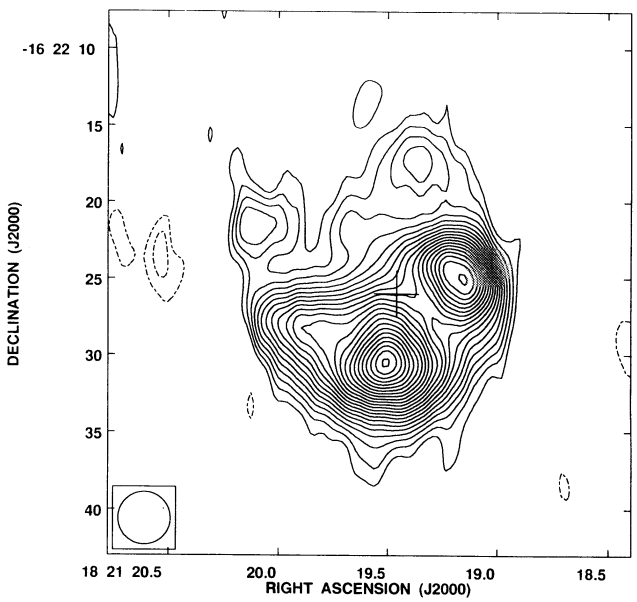

FIG. 18.—Contour map of 8.64 GHz emission of HD 168625. Contour intervals are −0.24, −0.16, 0.16, 0.24, 0.32, 0.40, 0.48, 0.56, 0.64, 0.72, 0.80, 0.88, 0.96, 1.04, 1.12, 1.20, 1.28, 1.36, 1.44, 1.52, 1.60, 1.68, 1.76, 1.84, and 1.92 mJy beam area^{-1}. The image has been restored with a circular beam of 3.″4, as shown in the lower left corner. The cross marks the optical position. The source is extended over a region of total extent ∼20″ × 18″, measured north-south by east-west. The strongest emission occurs from two components located 4.″5 west ("Source 1" in Table 2) and 4.″5 to the south (Source 2).

Hz. Equation (3) is accurate to within a few percent for the parameter space of interest (see Leitherer & Robert 1991). At centimeter wavelengths equation (3) becomes $g_\nu \propto \nu^{-0.1}$ so that the characteristic thermal radio spectrum of a hot star undergoing mass loss has a frequency dependence of $S_\nu \propto \nu^{0.6}$.

Equation (1) is applicable to isothermal, spherically symmetric, stationary, optically thick winds flowing at constant velocity. If one or more of these conditions are not met, the radio spectrum will deviate from a spectral index of 0.6. Leitherer & Robert (1991) studied the influence of temperature gradients, recombination zones, acceleration zones, geometries, and inhomogeneities on the resulting spectral index. In general, these effects can modify α by not more than ∼0.1.

Larger deviations from an $\alpha = 0.6$ spectrum occur if additional emission mechanisms, such as nonthermal processes, contribute. The survey of northern early-type stars conducted by Bieging et al. (1989) showed that 24% of the northern sources had a nonthermal contribution. Application of equation (1) to objects which have a significant nonthermal component in their radio flux will lead to an overestimate of the mass-loss rate. Several tests for distinguishing thermal from nonthermal emission exist (see Abbott 1985). The most conclusive test is the determination of the visibility function from an interferometer measurement at very high signal-to-noise ratio. Comparison with thermal wind models allows the detection of a possible nonthermal component. Nonthermal sources are unresolved and would require a brightness temperature much higher than the stellar temperature if they were interpreted in terms of thermal emission. Very few early-type stars are strong enough radio emitters for this experiment. White & Becker (1982) resolved the 6 cm radio emission of P Cygni with the VLA and showed that its radial surface brightness distribution is consistent with a thermal wind model. The same result was found for the B hypergiant Cygnus OB2 No. 12 (White & Becker 1983) and for the W-R star γ_2 Velorum (Hogg 1985). In contrast, White & Becker (1983) derived an electron temperature in excess of 300,000 K for Cygnus OB2 No. 9 (O5 If),

TABLE 1

POSITIONS AND MEASURED FLUX DENSITIES

Star	R.A.$^{optical}_{2000}$ [h m s]	Dec.$^{optical}_{2000}$ [° ′ ″]	R.A.$^{radio}_{2000}$ [h m s]	Dec.$^{radio}_{2000}$ [° ′ ″]	$S_\nu^{8.64}$ [mJy]	$S_\nu^{4.80}$ [mJy]
HD80077	09 15 54.74	−49 58 23.7	09 15 54.80	−49 58 24.8	0.50 ± 0.11	0.37 ± 0.10
HD86161	09 54 53.06	−57 43 39.1	09 54 52.91	−57 43 38.4	1.75 ± 0.09	1.21 ± 0.09
HD92740	10 41 17.56	−59 40 36.7	10 41 17.52	−59 40 36.9	1.50 ± 0.09	1.38 ± 0.13
HD93131	10 43 52.26	−60 07 03.8	10 43 52.26	−60 07 04.2	1.04 ± 0.09	0.35 ± 0.13
HD93162	10 44 10.47	−59 43 10.6	10 44 10.39	−59 43 11.0	0.90 ± 0.15	< 1.89
HD93250	10 44 45.13	−59 33 54.2	10 44 45.05	−59 33 54.7	1.36 ± 0.17	< 3.57
HD96548	11 06 17.25	−65 30 34.7	11 06 17.20	−65 30 35.2	2.52 ± 0.09	1.69 ± 0.10
HD152386	16 55 06.47	−44 59 20.9	–	–	< 0.3	< 0.3
LSS4065	17 19 00.49	−38 48 52.5	17 19 00.53	−38 48 51.3	2.99 ± 0.10	1.94 ± 0.19
HD160529	17 41 58.88	−33 30 12.8	17 41 59.03	−33 30 13.7	5.08 ± 0.11	3.82 ± 0.10
HD168607	18 21 14.77	−16 22 32.1	18 21 14.90	−16 22 32.2	0.85 ± 0.12	< 1.65
HD168625	18 21 19.46	−16 22 26.0	–	–	–	–

TABLE 2

8.64 GHz DATA OF THE RESOLVED EMISSION AROUND HD 168625

Parameter	Source 1	Source 2
R.A.$^{radio}_{2000}$ [h m s]	18 21 19.15	18 21 19.50
Dec.$^{radio}_{2000}$ [° ′ ″]	−16 22 25.0	−16 22 30.4
Peak flux [mJy/beam area]	1.5	1.9

suggesting that its radio properties are dominated by nonthermal processes.

If the stars are too weak to measure the visibility function at high signal-to-noise ratio, the observed radio spectral index can be used as a means for discriminating between thermal and nonthermal sources. Early-type stars with nonthermal spectra have spectral indices $\alpha \leq 0$ (Abbott, Bieging, & Churchwell 1984; Bieging et al. 1989), which makes them easily distinguishable from the thermal $\alpha = 0.6$ spectrum. This test has become the standard method to detect a nonthermal component in the radio spectra of early-type stars.

Seven of the 11 sources detected at 8.64 GHz were also detected at 4.80 GHz (Table 1). We can use these seven objects to investigate the consistency between the observed radio spectrum and equation (1). We calculated the expected flux at 4.80 GHz from the observed flux at 8.64 GHz under the assumption of $S_\nu \propto \nu^{0.6}$. In Figure 19 we compare these predicted fluxes to the ones actually observed. The figure contains 10 data points: seven detections at 4.80 GHz, plus the upper limits for HD 93162, HD 93250, and HD 168607, which were only detected at 8.64 GHz but not at 4.80 GHz. HD 168625 was omitted. The detected 8.64 GHz flux from the resolved circumstellar nebula is not expected to have a spectral index corresponding to an optically thick wind. Good agreement between the observed and predicted fluxes is found for the seven detected sources, suggesting that the observed radio fluxes have predominantly thermal origin. A nonthermal contribution will flatten the radio spectrum, i.e., shifting the data points in Figure 19 horizontally to the right of the dashed line. The location of HD 93162, HD 93250, and HD 168607 in Figure 19 is consistent both with and without a nonthermal component in the radio flux. Our upper limits on $S_\nu^{4.80}$ are not strong enough to exclude the presence of nonthermal emission in these stars.

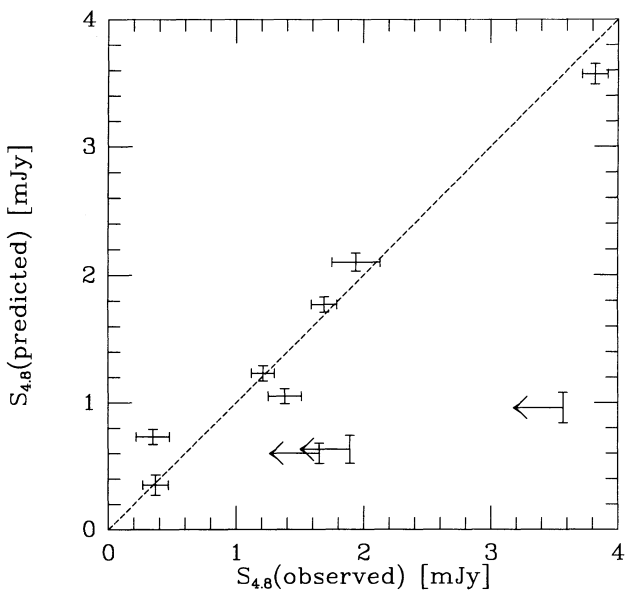

FIG. 19.—Predicted (ordinate) vs. observed (abscissa) 4.80 GHz fluxes. Predicted fluxes were calculated from the observed 8.64 GHz fluxes, assuming a spectral index of $\alpha = 0.6$. Nonthermal sources would be located to the right of the dashed line.

We conclude that for seven of the 11 sources (HD 80077, HD 86161, HD 92740, HD 93131, HD 96548, LSS 4065, and HD 160529), the radio emission is thermal in origin with only a small, if any, nonthermal contribution. Equation (1) is applicable and can be used to determine mass-loss ratios. For the three sources HD 93162, HD 93250, and HD 168607 the present data do not allow us to confirm whether the emission is thermal or otherwise. As we will discuss below, comparison with other, independent mass-loss estimators can provide additional constraints on the thermal versus nonthermal origin of the radio flux. Therefore, we will determine $\dot{M}$ for all 10 stars (and an upper limit for HD 152386) assuming the conditions for equation (1) are met and evaluate afterward if this assumption is indeed valid.

5. THE W-R STARS HD 86161, HD 92740, HD 93131, HD 93162, HD 96548, AND LSS 4065

The program stars form three natural groups in terms of their evolutionary status and wind parameters. HD 86161, HD 92740, HD 93131, HD 93162, HD 96548, and LSS 4065 are W-R stars of the nitrogen-rich WN subclass. Hamann, Koesterke, & Wessolowski (1993) and Crowther et al. (1995) did a comprehensive study of a large sample of Galactic W-R stars, including HD 86161, HD 92740, HD 93131, HD 93162, HD 96548, and LSS 4065 applying non-LTE models to optical observations. We take the stellar parameters of all six stars from these authors. For the reader's convenience, we give these cross-identifications: HD 86161 = WR 16, HD 92740 = WR 22, HD 93131 = WR 24, HD 93162 = WR 25, HD 96568 = WR 40, and LSS 4065 = WR 89. "WR" numbers refer to the catalog of W-R stars of van der Hucht et al. (1988).

Spectral types of the objects are given in column (2) of Table 3. This table summarizes all the adopted and derived stellar parameters. The stars form a homogeneous group of types WN7 and WN8. The four WN7 stars are established members of clusters, and their distances are relatively certain. The two WN8 stars are not members of clusters or associations. Crowther et al. (1995) derived photometric distances which we adopt here. The distances are in column (3) of Table 3. We assume that distances have an uncertainly of 20% if a star is an established member of a cluster, and 40% for a field star. This rule will also be used for the distance uncertainties of all other program stars.

Terminal wind velocities (col. [4] of Table 3) have been derived with different methods for all six stars. Prinja et al. (1990) utilized the saturated absorption troughs of strong ultraviolet lines, Eenens & Williams (1994) obtained v_∞ from infrared He I λ2.06 observations, and Crowther et al. (1995) and Hamann et al. (1993) performed fits to optical emission lines to derive v_∞. Crowther et al. critically reviewed the individual methods. We adopt their preferred values (their Table 10) and assume they are uncertain by 10%.

An estimate of the wind's electron temperature is required for the calculation of the Gaunt factor. Hillier's (1988, 1989) wind models suggest electron temperatures on the order of 10^4 K in the "radio" photospheres of W-R stars. Radio observations of the visibility function of a few hot stars indicate values ranging from 6000 K (Hogg 1985) to 20,000 K (White &

TABLE 3

ADOPTED AND DERIVED STELLAR WIND PARAMETERS[a]

Star	Spectral Type	d [kpc]	v_∞ [km s^{-1}]	T_e [K]	μ	Z	γ	$g_\nu^{8.64}$	log $\dot{M}$ [$M_\odot$ yr^{-1}]
HD80077	B2 Ia$^+$	3.0	140	5000	1.6	0.9	0.8	4.3	-5.62 ± 0.24
HD86161	WN8	3.2	630	10000	2.5	1.0	1.0	4.8	-4.44 ± 0.24
HD92740	WN7	2.6	1800	10000	1.7	1.0	1.0	4.8	-4.34 ± 0.16
HD93131	WN7	2.6	2200	10000	1.7	1.0	1.0	4.8	-4.38 ± 0.16
HD93162	WN7	2.6	2500	10000	1.5	1.0	1.0	4.8	(-4.41 ± 0.16)
HD93250	O3 V((f))	2.2	3200	20000	1.3	1.0	1.0	5.3	(-4.39 ± 0.15)
HD96548	WN8	3.3	840	10000	2.7	1.0	1.0	4.7	-4.15 ± 0.24
HD152386	O6: Iafpe	3.3	2000	10000	1.5	1.0	1.0	4.8	(< -4.47)
LSS4065	WN7	2.9	1600	10000	1.5	1.0	1.0	4.8	-4.14 ± 0.16
HD160529	B8 Ia$^+$	2.5	180	5000	1.6	0.9	0.8	4.3	-4.87 ± 0.24
HD168607	B9 Ia$^+$	2.2	140	5000	1.6	0.9	0.8	4.3	(-5.65 ± 0.16)

[a] Mass-loss rates in parentheses are for stars for which nonthermal emission at 8.64 GHz cannot be excluded.

Becker 1982). We adopt $T_e = 10{,}000$ K for all W-R stars (col. [5]). The actual choice of T_e is not critical for the derived $\dot{M}$ due to the weak temperature sensitivity of g_ν. For instance, varying T_e from 10,000 K to 20,000 K changes the mass-loss rate by only 5%.

The chemical abundances of W-R stars are of particular interest for the derivation of radio mass-loss rates. W-R stars can have He and heavy-element abundances which are sufficiently different from solar abundances so that the derived $\dot{M}$ becomes strongly dependent on the adopted chemical composition and ionization structure of the wind (see van der Hucht, Cassinelli, & Williams 1986). Fortunately this is a minor uncertainty for W-R stars of types WN6 and later. Elements heavier than helium are not overabundant enough to contribute either to μ or to the number of free electrons (see the review of Willis 1991). The values of μ, Z, and γ are solely determined by the relative H and He abundances. We calculated μ from the H/He ratios given by Crowther et al. (1995), except for LSS 4065, for which Hamann et al. (1993) quote an "extremely rich hydrogen contribution." Consequently, we adopted a helium overabundance relative to solar by a factor of 2 only (i.e., the same as for HD 152386; see § 6). Therefore, $\mu = 1.5$. The values for the mean molecular weight are in column (6) of Table 3. An uncertainty of 20% has been assumed.

Helium is singly ionized in the radio photospheres of WN7 and WN8 stars (van der Hucht et al. 1986; Willis 1991). This makes the calculation of the mean ionic charge and the number of free electrons per ion straightforward: $Z = 1.0$ and $\gamma = 1.0$ for all six stars (col. [7]). The uncertainties of these numbers are negligible.

Column (8) of Table 3 lists the resulting Gaunt factors at 8.64 GHz: $g_\nu^{8.64} = 4.8$ for all stars. We assign an uncertainty of 10% to $g_\nu^{8.64}$. This would result from an error of a factor of 2 in the adopted electron temperature.

Finally, column (9) summarizes the mass-loss rates derived with equation (1) using $S_\nu^{8.64}$. We preferred $S_\nu^{8.64}$ over $S_\nu^{4.80}$, since the observational errors of $S_\nu^{8.64}$ are generally smaller. The information provided by $S_\nu^{4.80}$ was already utilized in studying the spectral index. In addition, the errors in the derived mass-loss rates would not decrease if we had included the second measurement at 4.80 GHz, since the measurement errors of the radio fluxes are less important than other errors.

All six W-R stars have essentially identical mass-loss rates of $\dot{M} \approx 10^{-4.3 \pm 0.15}\ M_\odot\ \mathrm{yr}^{-1}$. The errors of individual mass-loss determinations are about 0.2 dex. They were calculated from the errors of all parameters entering in equation (1). The distance uncertainty is the single most important source of error. This can be seen from the bimodal distribution of the errors for $\dot{M}$. $\delta\dot{M}$ is smaller than 0.2 dex for W-R stars in clusters, and larger for field stars.

6. THE Of STARS HD 93250 AND HD 152386

Next we will discuss the two Of stars HD 93250 and HD 152386. Walborn (1971) first drew attention to the extremely early spectral type of HD 93250. The star belongs to the original group of stars defining spectral type O3. HD 93250 is a member of the cluster Trumpler 16. Despite numerous studies, its distance is still somewhat uncertain, mainly because of indications for an anomalous extinction law (see the extensive review given by Walborn 1995). Following Walborn (1995), we adopt $d = 2.2$ kpc, with a 20% uncertainty. The distance agrees with the distance of η Carinae recently derived by Allen & Hillier (1993) and corresponds to a ratio of the total to selective extinction of $R = 4$.

The classification of HD 93250 as O3 V((f)) suggests an extremely massive star. A detailed non-LTE analysis by Kudritzki (1980) and Kudritzki et al. (1992) indeed leads to $M = 100\ M_\odot$, making HD 93250 one of the most massive stars known in our Galaxy. Further evidence for a high mass comes from the observed high wind velocity of $v_\infty = 3200$ km s^{-1} (Groenewegen, Lamers, & Pauldrach 1989; Prinja et al. 1990; Kudritzki et al. 1992), since v_∞ correlates with the surface escape velocity, and therefore with mass. As we did for the W-R stars, an uncertainty of 10% is assumed for v_∞ (col. [4] of Table 3).

Kudritzki et al. (1992) found an effective temperature of 51,000 K for HD 93250. Drew's (1989) thermal equilibrium models for O-star winds predict a significant temperature decrease from the optical to the radio photosphere. Her models suggest $T_e \approx 0.4 T_{\mathrm{eff}}$. This leads to $T_e = 20{,}000$ K (col. [5]). Again we emphasize the weak dependence of $\dot{M}$ on T_e.

HD 93250 is an unevolved star still close to the main sequence. Its helium abundance is solar (Kudritzki et al. 1991), and therefore $\mu = 1.3$ with a 10% uncertainty. HD 93250 is extremely hot, making He^{++} the dominant ionization state close to the stellar surface. The radio-emitting region is several hundred stellar radii farther out, and helium can recombine from He^{++} to He^+ before the flow reaches the radius of the radio photosphere. This effect has been investigated in the Of4

star ζ Puppis by Pauldrach et al. (1994). If helium is singly ionized, we have $Z = \gamma = 1.0$. A 10% uncertainty accounts for the presence of some He^{++} in the radio-emitting region.

With $T_e = 20{,}000$ K and $Z = 1.0$, a Gaunt factor of 5.3 is found (col. [9] of Table 3).

The resulting 8.64 GHz mass-loss rate is $\dot{M} = 10^{-4.39 \pm 0.15}$ $M_\odot$ yr^{-1}. Anticipating the discussion in § 8, we remind the reader that this is the formal value derived under the assumption of a pure thermal emitter. No measurement of $S_\nu^{4.80}$ is available for HD 93250. Therefore we list the mass-loss rate of HD 93250 (and of all other stars without 4.80 GHz fluxes) in Table 3 in parentheses.

HD 152386 has received relatively little attention. Its spectral type is O6:Iafpe (Walborn 1982). Walborn (1973) noted the close spectral similarity between HD 152386 and the extensively studied star HD 152408. The close relation between HD 152386 and other luminous Of stars was also noted by Leep (1978). The main reason for the scarcity of observational data is the high reddening, which makes it difficult to observe the star in the blue and ultraviolet.

HD 152386 is not known to be a member of a cluster or OB association. Kozok's (1985) *UBV* data can be used to derive a photometric and spectroscopic distance. Assuming a normal reddening law with $R = 3.1$, we find a reddening-free visual magnitude of $V_0 = 5.62$. It is reasonable to adopt a similar absolute magnitude for HD 152386 as for its spectroscopic counterpart HD 152408, which has $M_V = -7.0$ (Crowther et al. 1995). This leads to a distance of 3.3 kpc. As we did for W-R field stars, we assign an uncertainty of 40% to this distance.

The heavy extinction toward HD 152386 precludes any v_∞ determination from ultraviolet resonance lines. We resort to the average wind velocity observed in luminous mid-O stars. Prinja et al. (1990) published a breakdown of terminal wind velocities for different spectral types and luminosity classes. We use their results to estimate $v_\infty = 2000 \pm 500$ km s^{-1} for HD 152386.

The remaining wind parameters in equation (1) are less crucial for the derivation of $\dot{M}$. We adopt $T_e = 10{,}000$ K, $\mu = 1.5$, $Z = \gamma = 1.0$ (see Table 3), with the same uncertainties as for HD 93250. The mean molecular weight, ionic charge, and number of electrons per ion are the same as for HD 152408 (Leitherer & Robert 1991). They reflect a helium overabundance by a factor of 2 and He^+ as the dominant ionization state.

The upper limit for the mass-loss rate is $\dot{M} = 10^{-4.47}$ $M_\odot$ yr^{-1}. The value is based on the upper limit of $S_\nu^{8.64}$ in Table 1 and includes the 1 σ errors of the stellar parameters discussed before. This is not a very strong limit on the mass-loss rate, but it is consistent with HD 152386 being a luminous O star at a relatively large distance.

7. THE B HYPERGIANTS HD 80077, HD 160529, AND HD 168607

HD 80077, HD 160529, and HD 168607 are extremely luminous B supergiants (designated B hypergiants by De Jager 1984). Their spectral types are B2 Ia^+ (HD 80077), B8 Ia^+ (HD 160529), and B9 Ia^+ (HD 168607). The three stars are close to—or have even entered—the LBV stage. Carpay et al. (1989), Carpay, De Jager, & Nieuwenhuijzen (1991), Sterken et al. (1991), and van Genderen et al. (1992) published detailed discussions of one or more of the three objects. We will base our adopted parameters largely on their results.

Only HD 168607 has a well-established distance. It is a member of the Serpens OB1 association at a distance of 2.2 kpc (Humphreys 1978). HD 160529 is a field star with a spectroscopic distance of 2.5 kpc (Sterken et al. 1991). This distance is based on the reasonable assumption that HD 160529 has the same absolute magnitude as its LMC counterpart R110. The distance of HD 80077 is still an open issue. Its spectroscopic parallax of 3 kpc places it at the distance of the open cluster Pismis 11. Therefore, it is likely that HD 80077 is a member of this cluster. Carpay et al. (1991) present a thorough discussion of the arguments for and against cluster membership and conclude that HD 80077 is indeed a member of Pismis 11. We adopt their distance of 3 kpc but conservatively assign an uncertainty of 40%, as appropriate for field stars. The same uncertainty is assumed for the distance of HD 160529, whereas for HD 168607 we take a value of 20%.

The wind opacity in the lowest Balmer lines of cool (as compared to O and W-R stars) B hypergiants is high enough that the blueshifted absorptions can be used to determine v_∞. Terminal wind velocities derived in this way are given in column (4) of Table 3. The value for HD 168607 is taken from Chentsov (1980). An uncertainty of 20% is assumed. Velocities between 100 and 200 km s^{-1} are quite typical for such stars. They are an order of magnitude lower than for the other stars in our program. Note that low values of v_∞ greatly facilitate the detection of mass-losing stars at radio wavelengths, even if $\dot{M}$ is not particularly high (see eq. [1]).

The electron temperature in the radio photosphere of the related star Cygnus OB2 No. 12 (B5 Ia^+) has been measured to be $T_e = 5000$ K (White & Becker 1983). We assume the same value applies to the three hypergiants as well.

Little is known about the chemical composition of the three stars. Analyses of LBVs typically suggest helium overabundances by a factor of a few relative to the Sun (e.g., Langer et al. 1994 for P Cygni; Leitherer et al. 1994 for AG Carinae). Most likely, the three hypergiants have a chemical composition similar to other LBVs so that $\mu = 1.5$, with a possible error of 10%. Furthermore, we assume $Z = 0.09$ and $\gamma = 0.8$ to account for the fact that helium is predominantly neutral in the winds of these cool stars (again with a 10% uncertainty). Table 3 summarizes all quantities discussed in this paragraph.

HD 80077 and HD 168607 have rather similar mass-loss rates of $10^{-5.62 \pm 0.24}$ $M_\odot$ yr^{-1} and $10^{-5.65 \pm 0.16}$ $M_\odot$ yr^{-1}, respectively. The mass-loss rate of HD 160529 is much higher at $\dot{M} = 10^{-4.87 \pm 0.24}$ $M_\odot$ yr^{-1}.

8. IMPLICATIONS OF THE DERIVED MASS-LOSS RATES

8.1. *Revisions to the Mass-Loss Rates of WN Stars?*

How do the mass-loss rates for the Wolf-Rayet stars derived from radio fluxes compare with rates obtained from alternative methods? Contrary to the situation of OB stars, which have lower wind densities, mass-loss rates of W-R stars can accurately be determined from several partially independent techniques. Crowther et al. (1995) and Hamann et al. (1993) derived mass-loss rates from optical recombination lines for all six W-R stars in our sample. Their results are compared to our values in Table 4. If necessary, we scaled the mass-loss rates of these authors to the same distances and terminal wind velocities we used in Table 3. Barlow et al. (1981) deduced mass-loss rates from infrared fluxes for three stars in common with our sample. Their results, after scaling them into our system of d, v_∞, μ, Z, and γ, are included in Table 4 as well. The four data

TABLE 4

VALUES OF log $\dot{M}$ DERIVED WITH DIFFERENT METHODS[a]

Star	Crowther et al.	Hamann et al.	Barlow et al.	This Work
HD86161	−4.2	−4.5	–	−4.4
HD92740	−4.3	−4.2	−4.4	−4.3
HD93131	−4.3	−4.2	−4.4	−4.4
HD93162	−4.4	−4.5	−4.5	−4.4
HD96548	−4.0	−4.1	–	−4.2
LSS4065	–	−4.2	–	−4.1

[a] Values in $M_\odot$ yr^{-1}.

sets are in excellent agreement. In no case does any one method lead to a discrepant value of $\dot{M}$. We note that the agreement between the radio mass-loss rate of HD 93162 and $\dot{M}$ derived independently is evidence for the thermal nature of the 8.64 GHz flux.

The characteristic radius of the bremsstrahlung emission is

$$R_\nu = 4.0 \times 10^{17} T_e^{-1/2} (\gamma g_\nu)^{1/3} \left(\frac{\dot{M} Z}{\mu v_\infty \nu} \right)^{2/3} \quad (4)$$

(Panagia & Felli 1975; Wright & Barlow 1975). R_ν is in $R_\odot$, and T_e is in K; all other units are as in equation (1). Inserting typical values for the W-R stars from Table 3, one finds $R_\nu^{8.64} \approx 10^4\ R_\odot$. The radius of the optical photosphere in late WN stars is about 25 $R_\odot$ (Crowther et al. 1995; Hamann et al. 1993). Therefore, the radio emission at 8.64 GHz typically originates at about 500 stellar radii. Observations of the bremsstrahlung spectrum at shorter wavelengths probe regions closer to the stellar surface, since $R_\nu \propto \nu^{-2/3}$. The infrared observations of Barlow et al. (1981) were obtained at 10 μm. Equation (4) suggests that the 10 μm flux is emitted within a few stellar radii of the stellar surface. Note that this is a very crude estimate only. Equation (4) was derived under the assumption of constant outflow velocity and large optical depth. This assumption may no longer be be entirely correct at infrared wavelengths. In any case, infrared and radio data sample wind regions whose radial distance from the stellar surface differs by about 2 orders of magnitude.

Optical recombination lines are approximately coincident with the 10 μm emission in their radius of origin. The wind density of late WN stars is low enough to permit observations close to the hydrostatic photospheric radius (see Crowther et al. 1995; Hamann et al. 1993). Therefore, our radio observations at 8.64 GHz on the one hand and the infrared continuum and optical line data on the other provide support for an outflow model whose density structure is adequately described by a homogeneous, stationary outflow. We cannot rule out inhomogeneous wind models having large density contrasts. Such models have been proposed, e.g., by Moffat & Robert (1994), who found evidence for "clumps" moving outward in the wind. Depending on the density contrast and the filling factor, the presence of clumps may lead to an *overestimate* of $\dot{M}$ if equation (1) is used to derive mass-loss rates. The same argument, of course, applies to mass-loss rates determined from infrared fluxes and optical emission lines. In all cases, the measured flux is sensitive to the square of the wind density and therefore immediately affected by filling factors which are different from unity. The fact that all methods lead to similar mass-loss rates makes it less likely that significant clumping prevails—unless the density contrast an filling factor happens to be preserved over 2 orders of magnitude in stellar radius.

8.2. *Is the* 8.64 GHz *Flux of HD 93250 Thermal?*

The mass-loss rate of the O3 main-sequence star HD 93250 is identical to the average mass-loss rate of the WN sample. This is quite surprising. O stars have generally weaker winds than W-R stars—in particular, an object like HD 93250, which is not yet in the supergiant stage. Interestingly, HD 93250 and the O4 V((f)) star HD 164794 share the same characteristics: as we will show below, they have quite similar stellar parameters, and their radio fluxes are inconsistent with their Hα mass-loss rates.

Conti & Frost (1977) observed the Hα line of HD 93250 but did not measure its equivalent width. We estimate that HD 93250 and HD 164794 have about the same Hα equivalent width (see Fig. 4 of Conti & Frost). The wind properties of HD 164794 have been analyzed by Lamers & Leitherer (1993) utilizing its measured Hα strength. We performed an identical analysis for HD 93250 under the assumption that it has the same Hα equivalent width W(Hα) as HD 164794. Lamers & Leitherer showed that $\dot{M}$ and the Hα luminosity of the wind, L(Hα), are related by

$$\log \dot{M} = 0.5 \log L(\mathrm{H}\alpha) + \log v_\infty + 0.5 \log R - 0.5I - 0.5c(T_{\mathrm{eff}}) - 12.563\,, \quad (5)$$

where $\dot{M}$ is in $M_\odot$ yr^{-1}, L(Hα) is in $L_\odot$, v_∞ is in km s^{-1}, and R is in $R_\odot$. I is the distance-integrated velocity law which enters into the expression of the emission measure, and $c(T_{\mathrm{eff}})$ accounts for electron-temperature–dependent atomic quantities. I and $c(T_{\mathrm{eff}})$ were defined and discussed by Leitherer (1988). In Table 5 we compare all relevant parameters. The values for HD 164794 were taken from Lamers & Leitherer (1993). W_{net} is the net equivalent width after subtraction of the photospheric Hα and He II λ6560 contribution (see Lamers & Leitherer). We made the reasonable assumption that both contributions are the same in HD 164794 and HD 93250. L(Hα) of HD 93250 is based on $M_V = -6.55$, as derived by Kudritzki (1980). R is from Kudritzki as well. I and $c(T_{\mathrm{eff}})$ of HD 93250 correspond to spectral type O3 V.

We find $\dot{M} = 10^{-5.45}\ M_\odot$ yr^{-1} for HD 93250. As expected from their similar Hα equivalent widths, HD 93250 and HD 164794 have approximately the same Hα mass-loss rate. Puls et al. (1995) performed a detailed analysis of the Hα profile of HD 93250 and found $\dot{M} = 10^{-5.31}\ M_\odot$ yr^{-1}, supporting the very similar nature of the two stars. Even after allowing for an error of a factor of a few, the Hα and radio mass-loss rates of HD 93250 are discrepant. They differ by a factor of 10, which is clearly outside the observational errors.

In the absence of a 4.80 GHz measurement of HD 93250, the thermal nature of its radio flux still needs to be established. We speculate that the excessively high radio mass-loss rate is an

TABLE 5

Hα MASS-LOSS RATES OF HD 164794 AND HD 93250

Parameter	Unit	HD164794	HD93250
W_{net}	Å	1.1	1.1
M_V	mag	−6.10	−6.55
L(Hα)	$L_\odot$	1.9	2.8
v_∞	km s^{-1}	3000	3200
R	$R_\odot$	16	18
I	–	1.18	1.19
c(T_{eff})	–	−6.65	−6.70
log $\dot{M}$	$M_\odot$ yr^{-1}	−5.62	−5.45

artifact due to significant nonthermal emission at 8.64 GHz. HD 93250 may again parallel HD 164794 in this respect. HD 164794 was one of the very first O stars detected at 4.9 GHz by Abbott et al. (1981). Its radio flux was interpreted as being thermal, and a mass-loss rate was derived which differed substantially from the Hα rate. Abbott et al. (1984) subsequently realized the predominantly nonthermal character of the emission and revised the mass-loss rate of HD 164794 downward by a factor of 7. Further monitoring of HD 93250 at 8.64 GHz and other frequencies is required to test for the presence of a nonthermal component in HD 93250 as well.

8.3. *The Mass-Loss Mechanism of B Hypergiants and LBVs*

Hardly any reliable mass-loss rates of luminous B stars can be found in the literature. HD 80077 and HD 160529 belong to those few B stars for which $\dot{M}$ has been estimated from the Hα. The Hα profile of HD 80077 has extended wings due to scattering of Hα photons by thermal electrons in the wind. The strength of the wings can be used to derive the electron scattering optical depth in the wind (Bernat & Lambert 1978). Carpay et al. (1989) applied this technique to HD 80077 and found $\dot{M} = 5^{+10}_{-3} \times 10^{-6}\ M_\odot\ \mathrm{yr}^{-1}$. Uncertainties in the adopted velocity law are responsible for the large errors. The mass-loss rate derived from our radio measurements is $\dot{M} = 2.4^{+2.0}_{-1.1} \times 10^{-6}\ M_\odot\ \mathrm{yr}^{-1}$—a significant improvement over the previous estimate.

As we discussed previously, density inhomogeneities would lead to an overestimate of $\dot{M}$ if derived via equation (1). Most techniques to determine $\dot{M}$ in hot stars, including radio determinations, rely on emission mechanisms which depend on the wind density squared. Comparison of such techniques provides few constraints on filling factors (unless an argument can be made that different outflow zones are observed with different techniques—see above). One notable exception is the measurement of the electron scattering depth, which depends on density only linearly. In the presence of significant clumping, mass-loss rates based on the strength of electron scattering wings would be lower than mass-loss rates from, e.g., radio fluxes (Scuderi et al. 1994). The agreement between our value and that of Carpay et al. (1989) suggests that the filling factor cannot be significantly different from unity.

Carpay et al. (1989) noted the relatively low mass-loss rate of HD 80077. Based on its luminosity, a rate well in excess of $10^{-5}\ M_\odot\ \mathrm{yr}^{-1}$ would be expected. However, the error bars of Carpay et al.'s mass-loss rate were large enough to make $\dot{M}$ still consistent with typical values. Our new determination confirms their low value and at the same time excludes a rate significantly above $5 \times 10^{-6}\ M_\odot\ \mathrm{yr}^{-1}$.

The mass-loss rate of HD 160529 has been estimated from the observed Hα profile by Sterken et al. (1991). They found $\dot{M} \approx 10^{-5}\ M_\odot\ \mathrm{yr}^{-1}$, in agreement with our more accurate radio value of $\dot{M} = 1.3^{+1.0}_{-0.5} \times 10^{-5}\ M_\odot\ \mathrm{yr}^{-1}$.

For the sake of completeness, we add that we searched through the literature for a mass-loss determination of HD 168607. We found none.

We discussed earlier the uniformity of W-R mass-loss rates over a relatively large range of stellar parameters. O stars, in contrast, cover a wide range of $\dot{M}$. However, their rates are tightly correlated with stellar parameters. For instance, Lamers & Leitherer (1993) found

$$\log \dot{M} = 1.738 \log L - 1.352 \log T_{\mathrm{eff}} - 9.547\ , \qquad (6)$$

where $\dot{M}$ is in $M_\odot\ \mathrm{yr}^{-1}$, L is in $L_\odot$, and T_{eff} is in K. The range of validity of equation (6) is $5.0 < \log L < 6.4$ and $4.45 < \log T_{\mathrm{eff}} < 4.70$. This relation predicts $\dot{M}$ of O stars with an rms uncertainty of $\sigma = 0.23$. Two properties of O-star winds are worth noting here. (i) There is a strong positive correlation between L and $\dot{M}$, which is a direct consequence of radiation pressure being the driving mechanism. (ii) Apart from a relatively mild T_{eff} dependence, $\dot{M}$ does not scale strongly with any stellar parameter in addition to L. The three hypergiants in our sample clearly behave differently. Their luminosities are $2 \times 10^6\ L_\odot$ (HD 80077; Carpay et al. 1989), $4 \times 10^5\ L_\odot$ (HD 160625; Sterken et al. 1991), and $3 \times 10^5\ L_\odot$ (HD 168607; van Genderen et al. 1982). Obviously there is no simple relation between $\dot{M}$ and L. If this were the case, HD 80077 should have a higher mass-loss rate than HD 160529, whereas the opposite is observed.

Does this mean the mass-loss mechanism in B hypergiants differs from O stars? This need not necessarily be the case. Radiatively driven winds of B stars are very sensitive to the adopted stellar parameters (Panagia & Macchetto 1982). Even small temperature variations may lead to significantly different mass-loss rates in the temperature range occupied by B stars. Pauldrach & Puls (1990) discovered a theoretical bi-stability in the wind of P Cygni which changes $\dot{M}$ by up to a factor of 3 for luminosity differences of only a few percent. Observational mass-loss rates of B stars are still too sparse for a comprehensive comparison with theory in this part of the Hertzsprung-Russell diagram. The few results obtained so far suggest that the winds of B stars are far more complex than the O-star species.

9. CONCLUSIONS

The results of this pilot study suggest that a significant number of hot luminous stars have 3 cm flux densities high enough to be observable with the Australia Telescope Compact Array. We are encouraged by the success of this program to extend the observations to a larger, statistically more significant sample of hot stars. Several key issues can be addressed with such a project.

(i) What is the fraction of nonthermal emitters among hot, luminous stars? Currently statistics are rather poor, in particular for O stars. Presently the nature of nonthermal radio emission from hot stars is not understood. Since nonthermal emission is often variable in time, frequency monitoring may establish timescales and help place constraints on existing theoretical models.

(ii) Few reliable mass-loss rates of B stars exist. Although $\dot{M}$ of B stars is generally lower than for O stars, the expected 8.64 GHz flux densities of O and B stars may actually be comparable. This is due to the much lower wind velocities in B-star winds. Correlating radio mass-loss rates and photospheric parameters of B stars may lead to evidence for driving forces other than radiation pressure in these winds.

(iii) Radio observations of W-R winds provide the unique opportunity to probe the chemistry and ionization state with very few model assumptions. In contrast to the WNL sample observed in the present program, hotter W-R stars, and in particular WC stars, are much more complex and far less understood in that respect. Comparison with the results of recombination-line studies allows tests of the ionization stratification in the wind. Such studies have been done for a few northern W-R stars before. The ATCA has the capability to increase the sample considerably.

Support for this work was provided by NASA through grant number GO-3605.02-91A. from the Space Telescope Science Institute, which is operated by the Association of Universities for Research in Astronomy, Incorporated, under NASA contract NAS5-26555. We thank Mike Potter for measuring the optical position of LSS 4065. Michael Dahlem's help and expert advice on AIPS is greatly appreciated. C. L. would like to express his gratitude to the staff at Narrabri and Sydney for the excellent support during the observations and the data reduction.

REFERENCES

Abbott, D. C. 1985, in Radio Stars, ed. R. M. Hjellming & D. M. Gibson (Dordrecht: Reidel), 61
Abbott, D. C., Bieging, J. H., & Churchwell, E. 1981, ApJ, 250, 645
———. 1984, ApJ, 280, 671
Abbott, D. C., Bieging, J. H., Churchwell, E., & Cassinelli, J. P. 1980, ApJ, 238, 196
Abbott, D. C., Bieging, J. H., Churchwell, E., & Torres, A. V. 1986, ApJ, 303, 239
Abbott, D. C., & Conti, P. S. 1987, ARA&A, 25, 113
Barlow, M. J., Smith, L. J., & Willis, A. J. 1981, MNRAS, 196, 101
Bernat, A., & Lambert, D. 1978, PASP, 90, 530
Bieging, J. H., Abbott, D. C., & Churchwell, E. 1989, ApJ, 340, 518
Carpay, J., De Jager, C., & Nieuwenhuijzen, H. 1991, A&A, 248, 475
Carpay, J., De Jager, C., Nieuwenhuijzen, H., & Moffatt, A. 1989, A&A, 216, 143
Cassinelli, J. P., & Lamers, H. J. G. L. M. 1987, in Exploring the Universe with the *IUE* Satellite, ed. Y. Kondo (Dordrecht: Reidel), 139
Chentsov, E. L. 1980, Soviet Astron. Lett., 6, 199
Clark, B. G. 1980, A&A, 89, 377
Conti, P. S., & Frost, S. A. 1977, ApJ, 212, 728
Conti, P. S., & Underhill, A. B. 1988, O Stars and Wolf-Rayet Stars (NASA SP-497)
Crowther, P. A., Smith, L. J., Hillier, D. J., & Schmutz, W. 1995, A&A, in press
Davidson, K. 1989, in IAU Colloq. 113, Physics of Luminous Blue Variables, ed. K. Davidson, A. F. J. Moffat, & H. J. G. L. M. Lamers (Dordrecht: Kluwer), 101
Davidson, K., Moffat, A. F. J., & Lamers, H. J. G. L. M., eds. 1989, IAU Colloquium 113, Physics of Luminous Blue Variables (Dordrecht: Kluwer)
De Jager, C. 1984, A&A, 138, 246
Drew, J. E. 1989, ApJS, 71, 267
Eenens, P. R. J., & Williams, P. M. 1994, MNRAS, 269, 1082
Garmany, C. D., Olson, G. L., Conti, P. S., & Van Steenberg, M. E. 1981, ApJ, 250, 660
Groenewegen, M. A. T., Lamers, H. J. G. L. M., & Pauldrach, A. W. A. 1989, A&A, 221, 78
Hamann, W.-R. 1994, in Evolution of Massive Stars, ed. D. Vanbeveren, W. van Rensbergen, & C. de Loore (Dordrecht: Kluwer), 237
Hamann, W.-R., Koesterke, L., & Wessolowski, U. 1993, A&A, 274, 397
Hillier, D. J. 1988, ApJ, 327, 822
———. 1989, ApJ, 347, 392
Högbom, J. 1974, ApJS, 15, 417
Hogg, D. E. 1985, in Radio Stars, ed. R. M. Hjellming & D. M. Gibson (Dordrecht: Reidel), 117
Humphreys, R. M. 1978, ApJS, 38, 309
Hutsemékers, D., Van Drom, E., Gosset, E., & Melnick, J. 1994, A&A, 290, 906
Israel, F. P., & Kennicutt, R. C. 1980, Astrophys. Lett., 21, 1
Kozok, J. R. 1985, A&AS, 61, 387
Kudritzki, R. P. 1980, A&A, 85, 174
Kudritzki, R. P., Gabler, R., Kunze, D., Pauldrach, A. W. A., & Puls, J. 1991, in Massive Stars in Starbursts, ed. C. Leitherer, N. R. Walborn, T. M. Heckman, & C. A. Norman (Cambridge: Cambridge Univ. Press), 59
Kudritzki, R. P., Hummer, D. G., Pauldrach, A. W. A., Puls, J., Najarro, F., & Imhoff, J. 1992, A&A, 257, 655
Lamers, H. J. G. L. M. 1981, ApJ, 245, 593
Lamers, H. J. G. L. M., & Groenewegen, M. A. T. 1990, in Properties of Hot Luminous Stars, ed. C. D. Garmany (Provo: Brigham Young Univ.), 189
Lamers, H. J. G. L. M., & Leitherer, C. 1993, ApJ, 412, 771
Langer, N., Hamann, W.-R., Lennon, M., Najarro, F., Pauldrach, A. W. A., & Puls, J. 1994, A&A, 290, 819
Leep, E. M. 1978, ApJ, 225, 165
Leitherer, C. 1988, ApJ, 326, 356
Leitherer, C., et al. 1994, ApJ, 428, 292
Leitherer, C., & Robert, C. 1991, ApJ, 377, 629
Maeder, A. 1994, in Evolution of Massive Stars, ed. D. Vanbeveren, W. van Rensbergen, & C. de Loore (Dordrecht: Kluwer), 349
Moffat, A. F. J., & Robert, C. 1994, ApJ, 421, 310
Olnon, F. M. 1975, A&A, 39, 217
Panagia, N., & Felli, M. 1975, A&A, 39, 1
Panagia, N., & Machetto, F. 1982, A&A, 106, 266
Pauldrach, A. 1987, A&A, 183, 295
Pauldrach, A. W. A., Kudritzki, R. P., Puls, J., Butler, K., & Hunsinger, J. 1994, A&A, 283, 525
Pauldrach, A. W. A., & Puls, J. 1990, A&A, 237, 409
Prinja, R. K., Barlow, M. J., & Howarth, I. D. 1990, ApJ, 361, 607
Puls, J., et al. 1995, A&A, submitted
Russell, J. L., Lasker, B. L., McLean, B. J., Sturch, C. R., & Jenkner, H. 1990, AJ, 99, 2059
Schaerer, D., & Schmutz, W. 1994, A&A, 288, 231
Scuderi, S., Bonanno, G., Spadaro, D., Panagia, N., Lamers, H. J. G. L. M., & De Koter, A. 1994, ApJ, 437, 465
Sellmaier, F., Puls, J., Kudritzki, R. P., Gabler, A., Gabler, R., & Voels, S. A. 1994, A&A, 273, 533
Sterken, C., Gosset, E., Jüttner, A., Stahl, O., Wolf, B., & Axer, M. 1991, A&A, 247, 383
van der Hucht, K. A., Cassinelli, J. P., & Williams, P. M. 1986, A&A, 168, 111
van der Hucht, K. A., Hidayat, B., Admiranto, A. G., Supelli, K. R., & Doom, C. 1988, A&A, 199, 217
van Genderen, A. M., et al. 1992 A&A, 264, 88
Walborn, N. R. 1971, ApJ, 167, L31
———. 1973, AJ, 78, 1067
———. 1982, ApJ, 256, 452
———. 1995, in The Eta Carinae Region: A Laboratory of Stellar Evolution, ed. V. Niemela (Revista Mexicana de Astronomia y Astrofisica), in press
White, R. L., & Becker, R. H. 1982, ApJ, 262, 657
———. 1983, ApJ, 272, L19
Willis, A. J. 1991, in IAU Symp. 143, Wolf-Rayet Stars and Interrelations with Other Massive Stars in Galaxies, ed. K. A. van der Hucht & B. Hidayat (Dordrecht: Kluwer), 265
Willis, A. J., & Garmany, C. D. 1987, in Exploring the Universe with the *IUE* Satellite, ed. Y. Kondo (Dordrecht: Reidel), 157
Wright, A. E., & Barlow, M. J. 1975, MNRAS, 170, 41